

Cite this: *RSC Adv.*, 2015, 5, 24750

# Limonoids from the root bark of *Dictamnus angustifolius*: potent neuroprotective agents with biometal chelation and halting copper redox cycling properties†

Jian-Bo Sun,<sup>†a</sup> Neng Jiang,<sup>†a</sup> Meng-Ying Lv,<sup>b</sup> Pei Wang,<sup>c</sup> Feng-Guo Xu,<sup>b</sup>  
Jing-Yu Liang<sup>\*a</sup> and Wei Qu<sup>\*a</sup>

Six novel limonoids, dictangustones A–F (1–6), along with four known limonoids were isolated from the root bark of *Dictamnus angustifolius*. The structures of the new limonoids were established by extensive 1D and 2D NMR spectroscopic experiments. *In vitro* studies show that all limonoids exhibited metal chelating property. Moreover, the Cu–ascorbate redox system assay revealed that the selected limonoid 2 could control Cu(I/II)-triggered hydroxyl radical (OH<sup>•</sup>) production by halting copper redox cycling via metal complexation. Importantly, the selected limonoids 1, 2, 4 and 6 were nontoxic to SH-SY5Y cells and showed significant neuroprotective activity against neuronal death induced by oxidative stress. Taken together, these limonoids such as limonoid 2 may be good candidates for developing new drugs in the treatment of neurodegenerative diseases, such as Alzheimer's disease and Parkinson's disease.

Received 7th January 2015  
Accepted 24th February 2015

DOI: 10.1039/c5ra00278h

www.rsc.org/advances

## 1. Introduction

Limonoids are a group of chemically related triterpenes derived from a precursor with a 4,4,8-trimethyl-17-furanosteroid skeleton.<sup>1</sup> The aglycones, such as limonin, nomilin, and obacunone, are bitter compounds with low water solubility that are found principally in Rutaceae and Meliaceae families.<sup>2,3</sup> Previous research on the potential health-promoting properties of limonoids concentrated on the growth regulating activity,<sup>4</sup> cancer-chemopreventive activity,<sup>5,6</sup> anti-inflammatory activity,<sup>7</sup> lowering cholesterol levels in blood,<sup>8</sup> cytotoxic activity,<sup>9–11</sup> anti-carcinogenic and antitumorogenic activity.<sup>12,13</sup> Recently, it has been predicated that limonoids from Rutaceae exhibited significant neuroprotective activities against glutamate-induced neurotoxicity in primary cultures of rat cortical cells<sup>14</sup> and human neuroblastoma cell line SH-SY5Y.<sup>15</sup> Obacunone was also

reported to be protective against glutamate-induced oxidative damage in mouse hippocampal HT22 cells.<sup>16</sup>

*Dictamnus angustifolius* (Rutaceae), distributed mainly in Xinjiang region of China, is a traditional Chinese medicine used to treat chronic hepatitis and jaundice.<sup>17–19</sup> A variety of components including limonoids,<sup>20</sup> quinoline alkaloids<sup>17</sup> and sesquiterpenes<sup>21</sup> were reported from this plant in recent years. Our previous investigation of the root bark of this plant has led to the isolation of three degraded limonoids, isodictamdiol A, dictamdiol and fraxinellone.<sup>22–24</sup> In a continuous effort to search for limonoids with structural and biological diversity from the root bark of *D. angustifolius*, six novel limonoids, dictangustones A–F (1–6), along with four known limonoids were isolated. Herein, we report the isolation and structural elucidation of dictangustones A–F (1–6). Moreover, their cell viability and neuroprotective capacity against oxidative stress were assayed using human neuroblastoma cell line SH-SY5Y.

## 2. Experimental

### 2.1. General

Optical rotations were measured using a JASCO P-1020 polarimeter. IR spectra were recorded on a Bruker Tensor 27 spectrometer using KBr disks. UV spectra were recorded with a Shimadzu UV-2450PC UV-vis spectrophotometer. NMR spectra were obtained using Bruker ACF-300 and ACF-500 NMR spectrometers. The chemical shift ( $\delta$ ) values are given in ppm with TMS as internal standard, and coupling constants ( $J$ ) in Hz. HRESIMS were measured with an Agilent 6520B Q-TOF mass

<sup>a</sup>Department of Natural Medicinal Chemistry, China Pharmaceutical University, Nanjing 210009, China. E-mail: jyliang08@126.com; popoqzh@126.com; Tel: +86 13605154996, +86 13852294378

<sup>b</sup>Key Laboratory of Drug Quality Control and Pharmacovigilance (Ministry of Education), China Pharmaceutical University, Nanjing 210009, China

<sup>c</sup>Center of Excellence in Post-Harvest Technologies, North Carolina Agricultural and Technical State University, North Carolina Research Campus, Kannapolis 28081, North Carolina, USA

† Electronic supplementary information (ESI) available. See DOI: 10.1039/c5ra00278h

‡ These authors contributed equally to this work and should be regarded as co-first authors.

instrument. All solvents used were of anal. Grade (Tianjin Chemical Co., Ltd, Tianjin, China). Column chromatography (CC) separations were carried out using silica gel (200–300 mesh, Qingdao Marine Chemical Co., Ltd, Qingdao, China) and Sephadex LH-20 (40–75  $\mu\text{m}$ , Pharmacia Biotech AB, Uppsala, Sweden). Thin-layer chromatography was performed on silica gel GF<sub>254</sub> (Qingdao Marine Chemical Co., Ltd, Qingdao, China). Spots were detected on TLC under UV light or by heating after spraying with 5% vanilin in H<sub>2</sub>SO<sub>4</sub> (v/v).

## 2.2. Plant material

The root bark of *D. angustifolius* were collected from Xinjiang Altay Region in October 2010, and identified by Professor She-Ban Pu, Department of Medicinal Plants, China Pharmaceutical University. A voucher specimen (no. 20100507) was deposited in Department of Natural Medicinal Chemistry, China Pharmaceutical University.

## 2.3. Extraction and isolation

The air-dried root bark of *D. angustifolius* (18 kg) were soaked in 95% EtOH (120 L  $\times$  3) at room temperature and extracted under reflux three times (4 h each). The combined extracts were filtered and the solvent was evaporated *in vacuo* to obtain a brown crude extract (850 g). The extracts were further dissolved in water and partitioned with petroleum ether, CH<sub>2</sub>Cl<sub>2</sub> and *n*-BuOH, successively. The CH<sub>2</sub>Cl<sub>2</sub> fraction (150 g) was subjected to column chromatography (CC) over silica gel and eluted with a gradient of CH<sub>2</sub>Cl<sub>2</sub>–MeOH (80 : 0 to 1 : 1, v/v) to yield 7 fractions (F1–F7). F7 (35.5 g) was applied to a silica gel column eluted with CH<sub>2</sub>Cl<sub>2</sub>–MeOH (40 : 0 to 1 : 1, v/v) to produce 4 sub-fractions (F7a and F7d). The fraction F7b (13.4 g) obtained was subjected to Sephadex LH-20 (CH<sub>2</sub>Cl<sub>2</sub>–MeOH 1 : 1, v/v) and then purified by preparative TLC (PE–Me<sub>2</sub>CO, 3 : 1) to afford **1** (16 mg). F7c (6.5 g) was separated by CC over silica gel (CH<sub>2</sub>Cl<sub>2</sub>–MeOH, 60 : 0 to 1 : 1, v/v) and Sephadex LH-20 (CH<sub>2</sub>Cl<sub>2</sub>–MeOH 1 : 1, v/v), then purified by preparative TLC (PE–Me<sub>2</sub>CO, 2 : 1) to give **2** (11 mg), **6** (12 mg) and **7** (23 mg). F7a (7.8 g) was applied to a silica gel column (PE–Me<sub>2</sub>CO, 15 : 1 to 1 : 1, v/v) to obtain 3 subfractions (F7a1–F7a3), F7a1 (4.4 g) was subjected to repeated CC over silica gel (CH<sub>2</sub>Cl<sub>2</sub>–MeOH, 40 : 0 to 1 : 1, v/v), Sephadex LH-20 and further purification by preparative TLC to afford **3** (15 mg) and **4** (28 mg). F1 (56.3 g) was separated by CC over silica gel (PE–EtOAc, 20 : 1 to 1 : 1, v/v) to yield **5** (18 mg) and four subfractions F1a–F1d. F1b (15.6 g) was subjected to CC over silica gel (CH<sub>2</sub>Cl<sub>2</sub>–MeOH, 40 : 0 to 1 : 1, v/v; Sephadex LH-20) to give **8** (21 mg), **9** (12 mg) and **10** (58 mg).

**2.3.1. Dictangustone A (1).** Amorphous white powder;  $[\alpha]_{25}^D$  –62.9° (c 0.10, MeOH); UV (MeOH)  $\lambda_{\text{max}}$  (log  $\epsilon$ ): 243 (3.36) nm; IR (KBr)  $\nu_{\text{max}}$ : 3444, 1712, 1639, 1399, 876 cm<sup>–1</sup>; for <sup>1</sup>H and <sup>13</sup>C NMR spectroscopic data, see Tables 1 and 2; HRESIMS  $m/z$  471.2023 [M – H]<sup>–</sup> (calcd for [C<sub>26</sub>H<sub>31</sub>O<sub>8</sub>]<sup>–</sup>, 471.2019).

**2.3.2. Dictangustone B (2).** Yellowish oil;  $[\alpha]_{25}^D$  –44.2° (c 0.10, MeOH); IR (KBr)  $\nu_{\text{max}}$ : 3444, 1742, 1709, 1639, 1225, 1026, 604 cm<sup>–1</sup>; for <sup>1</sup>H and <sup>13</sup>C NMR spectroscopic data, see Tables 1 and 2; HRESIMS  $m/z$  575.2506 [M – H]<sup>–</sup> (calcd for [C<sub>30</sub>H<sub>39</sub>O<sub>11</sub>]<sup>–</sup>, 575.2498).

**2.3.3. Dictangustone C (3).** Yellowish oil;  $[\alpha]_{25}^D$  –12.7° (c 0.10, MeOH); IR (KBr)  $\nu_{\text{max}}$ : 3444, 1752, 1705, 1633, 1399, 873 cm<sup>–1</sup>; for <sup>1</sup>H and <sup>13</sup>C NMR spectroscopic data, see Tables 1 and 2; HRESIMS  $m/z$  471.2028 [M – H]<sup>–</sup> (calcd for [C<sub>26</sub>H<sub>31</sub>O<sub>8</sub>]<sup>–</sup>, 471.2024).

**2.3.4. Dictangustone D (4).** Yellowish oil;  $[\alpha]_{25}^D$  –5.3° (c 0.10, MeOH); IR (KBr)  $\nu_{\text{max}}$ : 3438, 3347, 1745, 1731, 1636, 1402, 874 cm<sup>–1</sup>; for <sup>1</sup>H and <sup>13</sup>C NMR spectroscopic data, see Tables 1 and 2; HRESIMS  $m/z$  493.1821 [M + Na]<sup>+</sup> (calcd for [C<sub>26</sub>H<sub>30</sub>O<sub>8</sub>Na]<sup>+</sup>, 493.1833).

**2.3.5. Dictangustone E (5).** Yellowish oil;  $[\alpha]_{25}^D$  –5.0° (c 0.10, MeOH); IR (KBr)  $\nu_{\text{max}}$ : 3426, 1752, 1706, 1627, 1399, 873 cm<sup>–1</sup>; for <sup>1</sup>H and <sup>13</sup>C NMR spectroscopic data, see Tables 1 and 2; HRESIMS  $m/z$  493.1826 [M – H<sub>2</sub>O + Na]<sup>+</sup> (calcd for [C<sub>26</sub>H<sub>30</sub>O<sub>8</sub>Na]<sup>+</sup>, 493.1833).

**2.3.6. Dictangustone F (6).** Red brown oil;  $[\alpha]_{25}^D$  –11.4° (c 0.10, MeOH); IR (KBr)  $\nu_{\text{max}}$ : 3508, 1741, 1709, 1398, 877 cm<sup>–1</sup>; for <sup>1</sup>H and <sup>13</sup>C NMR spectroscopic data, see Tables 1 and 2; HRESIMS  $m/z$  437.1925 [M + Na]<sup>+</sup> (calcd for [C<sub>24</sub>H<sub>30</sub>O<sub>6</sub>Na]<sup>+</sup>, 437.1935).

## 2.4. Spectrophotometric measurement of complex with Cu<sup>2+</sup> and Fe<sup>2+</sup>

The metal chelation assay was carried out by UV-vis spectrophotometer (200 to 500 nm) in methanol.<sup>25,26</sup> The difference in UV-vis spectra generated by complex formation was acquired by numerical subtraction of the spectra of the metal and limonoid alone (at the same concentration used in the complex) from the spectra of the complex. A constant quantity of limonoid **2** (25  $\mu\text{mol L}^{-1}$ ) was mixed with growing amounts of copper ion (2–50  $\mu\text{mol L}^{-1}$ ) and examined the difference in UV-vis spectra to explore the ratio of metal/ligand in the mixture.

## 2.5. Ascorbate studies

In addition to limonoid **2** (dissolved in methanol and diluted in PBS) and CuSO<sub>4</sub>, other solutions were mixed and diluted in a PBS (20 mM phosphate, 100 mM NaCl buffer) at pH 7.4 with a final volume of 200  $\mu\text{L}$ .<sup>27</sup> Each experiment was performed in triplicate. Hydroxyl radical production was calculated as the transformation of CCA into 7-hydroxy-CCA ( $\lambda_{\text{excitation}} = 395 \text{ nm}$ ,  $\lambda_{\text{emission}} = 450 \text{ nm}$ ). The general order of addition was: CCA (50  $\mu\text{M}$ ), copper (5  $\mu\text{M}$ ) or ligand (15  $\mu\text{M}$ ), and ascorbate (150  $\mu\text{M}$ ). All of the test solutions contained 0.1% methanol and 1  $\mu\text{M}$  desferriyl.

## 2.6. Cell culture and MTT assay for cell viability

Human SH-SY5Y neuroblastoma cells were maintained in 10% FBS (fetal bovine serum), Eagle's EMEM (minimum essential medium), Ham's F12 described by Reddy,<sup>28</sup> 100  $\mu\text{g mL}^{-1}$  streptomycin and 100 U mL<sup>–1</sup> penicillin in a humidified incubator at 37 °C in 5% CO<sub>2</sub> atmosphere. Cells were plated at  $1 \times 10^4$  cells per well in 96-well plates and allowed to adhere and grow. Limonoids **1**, **2**, **4** and **6** were added to the cultures after they were transplanted into serum when cells reached the required confluence.<sup>29</sup> To determine the cell viability, 20  $\mu\text{L}$  MTT was added to each well, and cells were cultured in

Table 1  $^1\text{H}$ -NMR spectroscopic data of compounds 1–6 ( $\delta_{\text{H}}$  in ppm,  $J$  in Hz)

Position	1 <sup>a</sup>	2 <sup>b</sup>	3 <sup>c</sup>	4 <sup>a</sup>	5 <sup>b</sup>	6 <sup>a</sup>
1	6.73 d (16.0)	4.83 d (6.2)	6.10 br s	4.09 m	4.10 br s	1.82 br s (2H)
2 $\alpha$	5.72 d (16.0)	3.14 m	5.77 d (13.4)	2.44 dd (4.5, 14.0)	2.86 dd (4.5, 18.1)	—
2 $\beta$	—	3.14 m	—	2.94 dd (13.6, 14.0)	2.99 br s	—
5	2.04 dd (4.5, 13.4)	2.47 d (13.0)	3.31 br s	—	2.79 dd (2.5, 16.4)	2.06 dd (6.9, 13.7)
6 $\alpha$	2.46 dd (13.6, 4.5)	2.11 br s	2.39 dd (4.5, 14.0)	5.72 s	—	2.59 dd (6.9, 13.2)
6 $\beta$	2.95 m	1.75 t (13.0)	3.07 t (14.0)	—	4.67 m	2.53 dd (8.0, 13.2)
7	—	4.47 s	—	—	—	—
9	3.33 d (11.1)	2.83 m	1.80 br s	1.73 s	2.70 dd (1.9, 13.0)	4.14 s
11 $\alpha$	1.70 m	1.63 d (11.2)	1.68–1.70 m	1.70–1.71 m	1.97 m	—
11 $\beta$	1.68 d (11.1)	1.75 d (14.5)	1.68–1.70 m	1.70–1.71 m	1.86 m	—
12 $\alpha$	1.45 m	1.50 m	1.21 br s	1.27 br s	1.73 m	5.72 s
12 $\beta$	1.71 m	1.65 dd (8.0, 11.2)	1.82 dd (7.9, 13.4)	1.21 br s	1.95 m	—
14	—	—	—	—	—	2.15 m
15	3.62 s	3.50 s	3.62 s	3.68 s	4.15 s	3.68–3.94 m (2H)
17	5.40 s	5.59 s	5.43 s	5.42 s	5.47 s	4.86 s
18	1.08 s	1.18 s	1.09 s	1.11 s	1.08 s	1.00 s
19	1.45 s	1.20 s	1.54 s	1.23 s	1.28 s	1.27 s
21	7.39 s	7.42 s	7.58 s	7.39 s	7.44 s	7.46 s
22	6.31 s	6.30 s	6.47 s	6.35 s	6.36 s	6.38 s
23	7.36 s	7.39 s	7.53 s	7.37 s	7.43 s	7.45 s
28	1.16 s	1.38 s	1.21 s	1.30 s	1.53 s	1.29 s
29	1.22 s	1.49 s	1.27 s	1.51 s	1.58 s	1.31 s
30	1.18 s	1.13 s	1.17 s	1.16 s	1.19 s	1.84 s
OH	—	—	2.92 br s (17-OH) 10.90 s (16-OH) <sup>d</sup>	4.14 m (1-OH)	4.15 br s (1-OH) 4.67 m (6-OH)	—
1-OAc	—	2.06 s	—	—	—	—
7-OAc	—	2.15 s	—	—	—	—

<sup>a</sup> Data were measured in  $\text{CDCl}_3$  at 300 MHz. <sup>b</sup> Data were measured in  $\text{CDCl}_3$  at 500 MHz. <sup>c</sup> Data were measured in  $\text{CD}_3\text{COCD}_3$  at 500 MHz. <sup>d</sup> Data was measured in  $\text{CD}_3\text{COCD}_3$  at 300 MHz.

additional incubation for 4 h, then cells containing MTT formazan crystals were dissolved with 200  $\mu\text{L}$  DMSO. The optical density was measured with a spectrophotometer (TECAN®, Spectra model Classic, Salzburg, Austria) at 570 nm. Results were expressed as the mean  $\pm$  SD of three independent tests.

### 2.7. Neuroprotective activity in SH-SY5Y cells

SH-SY5Y cells were seeded at  $1 \times 10^4$  cells per well in 96-well plates. After adhesion for 24 h, the growth medium was removed and replaced with the tested limonoids (1, 3, 5, 10  $\mu\text{M}$ ) and incubated for 24 h at 37  $^\circ\text{C}$  with  $\text{CO}_2$  in a humidified atmosphere. Then, the cells were incubated with 100  $\mu\text{M}$   $\text{H}_2\text{O}_2$  at 37  $^\circ\text{C}$  for 24 h before treated with MTT.<sup>30</sup> Trolox was used as the control with concentrations of 3  $\mu\text{M}$ . Results were expressed as percent viability compared to untreated cells.

## 3. Results and discussion

The root bark of *D. angustifolius* was extracted using 95% EtOH. The crude extract was suspended in water and extracted with petroleum ether,  $\text{CH}_2\text{Cl}_2$ , and BuOH, successively. The  $\text{CH}_2\text{Cl}_2$  extract was subjected repeatedly to silica gel, Sephadex LH-20, and preparative TLC to afford ten limonoids. The structures of the six previously unreported limonoids, termed dictangustones A–F (1–6), were elucidated by analysis using HRESIMS

and 1D and 2D NMR, including  $^1\text{H}$ - $^1\text{H}$  COSY, HSQC, HMBC, and ROESY experiments. The four known limonoids were identified by comparison of their MS and NMR data with those previously reported (Fig. 1).

### 3.1. Characterization of the limonoids

Limonoid 1 was obtained as amorphous powder. The HRESIMS spectrum yielded a quasimolecular ion of  $[\text{M} - \text{H}]^-$  at  $m/z$  471.2023 (calcd 471.2019), consistent with molecular formula of  $\text{C}_{26}\text{H}_{32}\text{O}_8$  and with 11 indices of unsaturation. The IR spectrum suggested the presence of hydroxyl ( $3444\text{ cm}^{-1}$ ) and carbonyl ( $1712\text{ cm}^{-1}$ ). The  $^1\text{H}$  and  $^{13}\text{C}$  NMR data (Tables 1 and 2) revealed the presence of one characteristic  $\beta$ -substituted furyl ring signals [ $\delta_{\text{H}}$  7.39, 7.36 and 6.31 (each 1H, s);  $\delta_{\text{C}}$  109.4, 119.8, 140.7, and 142.7]; one lactone ring oxygenated methenyl signals [ $\delta_{\text{H}}$  5.40 (1H, s);  $\delta_{\text{C}}$  78.3]; one characteristic epoxy proton  $\delta_{\text{H}}$  3.62 (1H, s); one (*E*)-olefinic group [ $\delta_{\text{H}}$  5.72 and 6.73 (each 1H, d,  $J = 16.0\text{ Hz}$ );  $\delta_{\text{C}}$  119.8 and 160.6]; five methyl signals [ $\delta_{\text{H}}$  1.08, 1.45, 1.16, 1.22 and 1.18 (each 3H, s);  $\delta_{\text{C}}$  20.5, 19.8, 29.1, 30.4 and 29.2]. These NMR data were similar to those of obacunoic acid<sup>31</sup> except that the coupling constant of the two protons was larger (16.0 Hz) in 1. This suggested that the coupling mode of the double bond was *trans* rather than *cis* in obacunoic acid. All protons directly bonded with carbon atoms and the planar structure was assigned by analysis of the  $^1\text{H}$ - $^1\text{H}$  COSY, HSQC,

**Table 2**  $^{13}\text{C}$ -NMR spectroscopic data for compounds 1–6 ( $\delta_{\text{C}}$  in ppm)

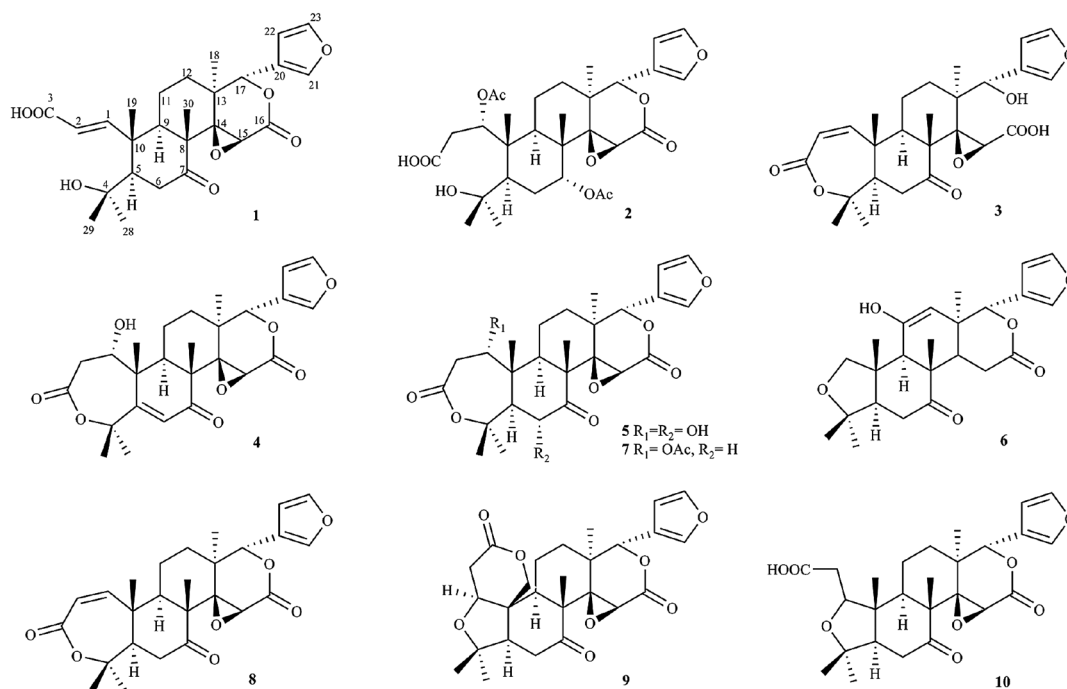
Position	1 <sup>a</sup>	2 <sup>b</sup>	3 <sup>c</sup>	4 <sup>a</sup>	5 <sup>b</sup>	6 <sup>a</sup>
1	160.6	70.6	156.8	60.7	79.1	30.9
2	119.8	34.9	119.2	38.1	34.8	—
3	168.0	169.7	165.5	166.2	169.1	—
4	72.8	85.1	73.2	78.2	81.8	68.3
5	59.3	43.9	56.0	150.1	53.3	31.8
6	37.3	25.7	38.7	118.6	68.5	33.0
7	210.8	73.1	210.6	209.5	195.2	199.0
8	52.6	41.9	53.6	52.7	48.4	54.1
9	48.7	36.7	49.4	45.7	46.3	60.4
10	44.8	44.7	46.6	45.2	46.8	44.4
11	32.3	25.8	33.5	32.7	31.7	130.7
12	19.8	14.9	20.4	19.5	20.5	100.7
13	37.3	38.7	38.2	37.4	37.3	29.5
14	65.4	69.6	66.3	65.5	65.3	45.3
15	52.8	56.7	53.9	53.3	52.1	64.5
16	168.5	167.3	167.7	167.3	166.4	163.1
17	78.3	78.3	78.8	73.5	77.8	81.5
18	20.5	16.7	20.9	20.4	20.5	19.1
19	19.8	15.8	20.4	29.0	29.7	29.7
20	119.0	120.3	121.8	120.3	119.7	121.0
21	140.7	141.1	142.2	140.8	141.1	140.2
22	109.5	109.7	111.0	109.8	109.6	108.7
23	142.8	143.1	144.0	142.9	143.3	143.2
28	29.1	34.3	33.5	32.4	25.7	30.7
29	30.4	23.6	31.9	19.2	25.2	24.8
30	29.2	18.3	16.7	16.5	18.1	15.0
1-OAc	—	169.6	—	—	—	—
—	—	20.8	—	—	—	—
7-OAc	—	169.8	—	—	—	—
—	—	21.0	—	—	—	—

<sup>a</sup> Data were measured in  $\text{CDCl}_3$  at 75 MHz. <sup>b</sup> Data were measured in  $\text{CDCl}_3$  at 125 MHz. <sup>c</sup> Data were measured in  $\text{CD}_3\text{COCD}_3$  at 125 MHz.

HMBC, and ROESY experiments (see ESI†). Thus, the structure of **1**, named dictangustone A, was identified as shown in Fig. 1.

Limonoid **2** was obtained as amorphous powder. The HRE-SIMS showed a  $[\text{M} - \text{H}]^-$  ion at  $m/z$  575.2506 (calcd for  $[\text{C}_{30}\text{H}_{39}\text{O}_{11}]^-$ , 575.2498), consistent with molecular formula of  $\text{C}_{30}\text{H}_{40}\text{O}_{11}$  and with 11 indices of unsaturation. The IR spectrum displayed absorption bands for a carboxylic acid group ( $3444$  and  $1709\text{ cm}^{-1}$ ) and saturated carbonyl groups ( $1742\text{ cm}^{-1}$ ). Its  $^1\text{H}$  and  $^{13}\text{C}$  NMR spectroscopic data (Tables 1 and 2) were very similar to those of odorlide<sup>32</sup> except for the absence of one acetyl group in C-11 and one methoxyl group in C-3. All protons directly bonded with carbon atoms were assigned by analysis of the HSQC spectrum. From the subsequent 2D NMR studies using  $^1\text{H}$ - $^1\text{H}$  COSY, HMBC and NOESY spectra, it was strongly suggested that **2** was an odorlide derivative. The HMBC correlation of methine protons ( $\delta_{\text{H}}$  4.83) with 1-OAc ( $\delta_{\text{C}}$  169.6), C-2 ( $\delta_{\text{C}}$  34.9) and C-19 ( $\delta_{\text{C}}$  15.8) suggested that the acetyl group was located at C-1. The location of another acetyl group was determined by the HMBC correlation of methine protons ( $\delta_{\text{H}}$  4.47) with 7-OAc ( $\delta_{\text{C}}$  169.8), C-8 ( $\delta_{\text{C}}$  41.9) and C-30 ( $\delta_{\text{C}}$  18.3). The low field shift of H-1 ( $\delta_{\text{H}}$  4.83) highly deshielded by the closely spaced 4-OH group and the ROESY correlations of H-1 ( $\delta_{\text{H}}$  4.83) with H-5 ( $\delta_{\text{H}}$  2.47), H-9 ( $\delta_{\text{H}}$  2.83) and 18- $\text{CH}_3$  ( $\delta_{\text{H}}$  1.18) along with the ROESY correlation of H-7 ( $\delta_{\text{H}}$  4.47) with 30- $\text{CH}_3$  ( $\delta_{\text{H}}$  1.13) (Fig. 2) suggested that the relative configuration of the two acetyl groups were both  $\alpha$ -orientations. Thus, the structure of **2**, named dictangustone B, was shown in Fig. 1.

Limonoid **3** was obtained as yellowish oil. The HRESIMS spectrum yielded a quasimolecular ion of  $[\text{M} - \text{H}]^-$  at  $m/z$  471.2028 (calcd 471.2024), consistent with molecular formula of  $\text{C}_{26}\text{H}_{32}\text{O}_8$  and with 11 indices of unsaturation. The IR spectrum

**Fig. 1** Structures of limonoids 1–10.



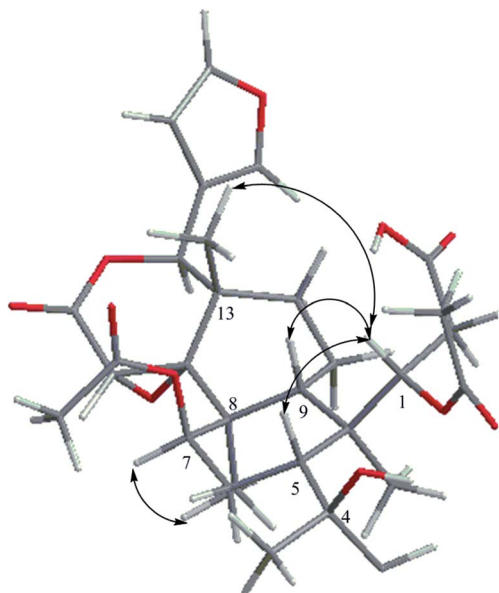


Fig. 2 Key ROESY correlations of limonoid 2.

suggested the presence of OH ( $3444\text{ cm}^{-1}$ ) and carbonyl ( $1752$  and  $1705\text{ cm}^{-1}$ ). Its  $^1\text{H}$  NMR and  $^{13}\text{C}$  NMR data (Tables 1 and 2) were similar to those of **1**, with the main differences being the resonances of the two olefinic protons at  $\delta_{\text{H}}$  6.10 (br s) and  $\delta_{\text{H}}$  5.77 (d,  $J = 13.4\text{ Hz}$ ) relative to the signals of a *cis* double bond in **3**. The HMBC correlation of hydroxyl proton ( $\delta_{\text{H}}$  2.92) with C-13 ( $\delta_{\text{C}}$  38.2) suggested that the structure of **3** was an obacunone derivative with D-ring cracking skeleton like nomilinoate A-ring lactone.<sup>33</sup> Thus, the structure of **3**, named dictangustone C, was identified as shown in Fig. 1.

Limonoid **4** was obtained as yellowish oil. Its HRESIMS showed a positive ion peak at  $m/z$  493.1821  $[\text{M} + \text{Na}]^+$  (calcd 493.1833), corresponding to a molecular formula of  $\text{C}_{26}\text{H}_{30}\text{O}_8$  and with 12 indices of unsaturation. The IR absorptions at 3438, 3347, 1745 and  $1731\text{ cm}^{-1}$  indicated the presence of hydroxyl and carbonyl groups. Its  $^1\text{H}$  and  $^{13}\text{C}$  NMR spectroscopic data (Tables 1 and 2) were similar to those of deacetylnomilin<sup>34,35</sup> except for the presence of one carbonyl conjugated olefinic group in **4** ( $\delta_{\text{H}}$  5.72 (1H, s);  $\delta_{\text{C}}$  118.6 and 150.1). The  $^1\text{H}$  and  $^{13}\text{C}$  NMR data of the main structural was assigned by analyses of data from  $^1\text{H}$ - $^1\text{H}$  COSY, HSQC, HMBC, and ROESY experiments and by comparison with those of deacetylnomilin. The HMBC correlation of olefinic protons ( $\delta_{\text{H}}$  5.72) with C-7 ( $\delta_{\text{C}}$  209.5) and C-4 ( $\delta_{\text{C}}$  78.2) suggested that the olefinic group was located at C-5 and C-6. The ROESY correlations of H-1 ( $\delta_{\text{H}}$  4.09) with 19- $\text{CH}_3$  ( $\delta_{\text{H}}$  1.23) and 29- $\text{CH}_3$  ( $\delta_{\text{H}}$  1.51), 1-OH ( $\delta_{\text{H}}$  4.14) with 9-H ( $\delta_{\text{H}}$  1.73) suggested that the relative configuration of the hydroxyl group was  $\alpha$ -orientation. Thus, the structure of **4**, named dictangustone D, was shown in Fig. 1.

Limonoid **5** was obtained as yellowish oil. The HRESIMS showed a positive ion peak at  $m/z$  493.1826  $[\text{M} - \text{H}_2\text{O} + \text{Na}]^+$  (calcd 493.1833), corresponding to a molecular formula of  $\text{C}_{26}\text{H}_{32}\text{O}_9$  and with 11 indices of unsaturation. The IR spectrum suggested the presence of OH ( $3426\text{ cm}^{-1}$ ) and carbonyl ( $1752$  and  $1706\text{ cm}^{-1}$ ) groups. The  $^1\text{H}$  NMR and  $^{13}\text{C}$  NMR data (Tables

1 and 2) of **5** were similar to those of deacetylnomilin<sup>35</sup> except for the presence of another hydroxyl group in C-6, which was determined by the HMBC correlation of methine protons H-6 ( $\delta_{\text{H}}$  4.67) with C-4 ( $\delta_{\text{C}}$  81.8) and C-7 ( $\delta_{\text{C}}$  195.2). The ROESY correlations of H-1 ( $\delta_{\text{H}}$  4.10) with 19- $\text{CH}_3$  ( $\delta_{\text{H}}$  1.28), 1-OH ( $\delta_{\text{H}}$  4.15) with H-5 ( $\delta_{\text{H}}$  2.79) and H-6 ( $\delta_{\text{H}}$  4.67) with 30- $\text{CH}_3$  ( $\delta_{\text{H}}$  1.19) suggested that the relative configuration of the two hydroxyl groups were both  $\alpha$ -orientations. Thus, the structure of **5**, named dictangustone E, was identified as shown in Fig. 1.

Limonoid **6** was obtained as red brown oil. The HRESIMS spectrum yielded an ion of  $[\text{M} + \text{Na}]^+$  at  $m/z$  437.1925 (calcd 437.1935) that together with the  $^{13}\text{C}$  NMR data indicated a molecular formula of  $\text{C}_{24}\text{H}_{30}\text{O}_6$  and with 10 indices of unsaturation. The IR spectrum suggested the presence of OH ( $3508\text{ cm}^{-1}$ ) and carbonyl ( $1741$  and  $1709\text{ cm}^{-1}$ ) groups. The  $^1\text{H}$  NMR and  $^{13}\text{C}$  NMR data (Tables 1 and 2) of **6** were similar to those of isoobacunonic acid<sup>31</sup> except for the absence of one acetic acid substituent and the presence of one enol structure in **6**. Its  $^1\text{H}$  and  $^{13}\text{C}$  NMR data of the main structure were assigned by analyses of data from  $^1\text{H}$ - $^1\text{H}$  COSY, HSQC, HMBC, and ROESY experiments. The HMBC correlations of olefinic proton H-12 ( $\delta_{\text{H}}$  5.72) with C-11 ( $\delta_{\text{C}}$  130.7) and C-17 ( $\delta_{\text{C}}$  81.5) suggested that the olefinic group was located at C-11 and C-12. The HMBC correlations of one hydroxyl proton ( $\delta_{\text{H}}$  8.5) with C-9 ( $\delta_{\text{C}}$  60.4) and C-12 ( $\delta_{\text{C}}$  100.7) indicated that the hydroxyl group was located at C-11. In addition, the chemical shift of C-9 ( $\delta_{\text{C}}$  60.4) at low field was due to highly deshielded by the closely spaced 11-OH. Thus, the structure of **6**, named dictangustone F, was shown in Fig. 1.

Four known limonoids (**7**–**10**) were identified by comparison of their MS and NMR spectroscopic data with literature as nomilin,<sup>36</sup> obacunone,<sup>37</sup> limonin<sup>38</sup> and isoobacunonic acid,<sup>31</sup> respectively. The complete  $^{13}\text{C}$  NMR assignments for nomilin (**7**) determined by 1D and 2D NMR analysis is first reported (see ESI†).

Previous research have indicated that excessive biometals (such as iron, zinc, and copper) exist in the brains of Alzheimer's disease (AD) patients are several-fold than the normal age-matched neuropil.<sup>39</sup> Redox-active metal ions, such as  $\text{Cu}^{2+}$  and  $\text{Fe}^{2+}$ , contribute to the production of reactive oxygen species (ROS)<sup>40,41</sup> and oxidative stress plays an important role in the pathogenesis of AD for it could be attributed to a high degree of neurotoxicity leading to neuronal death and ultimately, cognitive impairment.<sup>42</sup> Thus, metal chelating property and neuroprotection are valuable tools of modern medicine to potentially combat or slow down the progression of neurodegenerative conditions such as AD.<sup>43</sup>

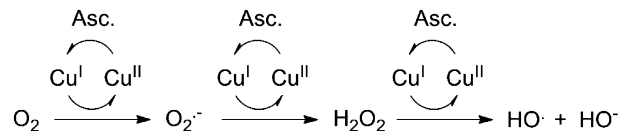
### 3.2. Metal chelating effect

The chelating effect of all isolated limonoids for metals such as  $\text{Cu}^{2+}$  and  $\text{Fe}^{2+}$  in methanol was measured by UV-vis spectrometry.<sup>25,26</sup> As a representative example, UV-vis spectra of limonoid **2** with increasing  $\text{Cu}^{2+}$  concentrations was observed as shown in Fig. 3a. The increase in absorbance, estimated by differential spectra (Fig. 3b), indicated that there was an interaction between limonoid **2** and  $\text{Cu}^{2+}$ . Similar behavior was also observed when using  $\text{Fe}^{2+}$ . These observations suggested that the isolated limonoids could effectively chelate  $\text{Cu}^{2+}$  and  $\text{Fe}^{2+}$ ,

and thus could be used as metal chelators in treating AD. The ratio of metal/ligand ion in the complex was observed by using the increasing ligand with fixed amount metal ion. The maximum intensity of different spectra was observed at almost 1 : 1, which indicated the stoichiometry of the complex.

### 3.3. The ability of halting copper redox cycling by metal complexation

As previous reported, redox-active Cu(II) is related to the generation of ROS, leading to the increasement of oxidative stress, which is one proposed neuropathology of AD. Therefore, the Cu-ascorbate redox system (Scheme 1) was used to determine if the limonoid 2 could halt copper ion based on the redox activity under aerobic conditions.<sup>27</sup> The generation of hydroxyl radicals (OH<sup>•</sup>) by copper redox cycling in the presence of ascorbate was detected by coinubation with coumarin-3-carboxylic acid (CCA), which produces fluorescent 7-hydroxy-CCA in the presence of OH<sup>•</sup>. As shown in Fig. 4, the OH<sup>•</sup> in



Scheme 1 Hydroxyl radical (OH<sup>•</sup>) production by copper redox cycling in the presence of ascorbate.

the copper-ascorbate system increased steadily with time, and achieved the highest at approximately 11 min. When limonoid 2 was coinubated with the Cu-ascorbate system, this procedure was halted almost entirely, which indicated that the ligand was able to halt the copper redox cycling involved in oxidative stress by metal complexation.

### 3.4. Cell viability and neuroprotection studies

To further study the therapeutic potential of these isolated limonoids, cell viability and neuroprotective capacity against

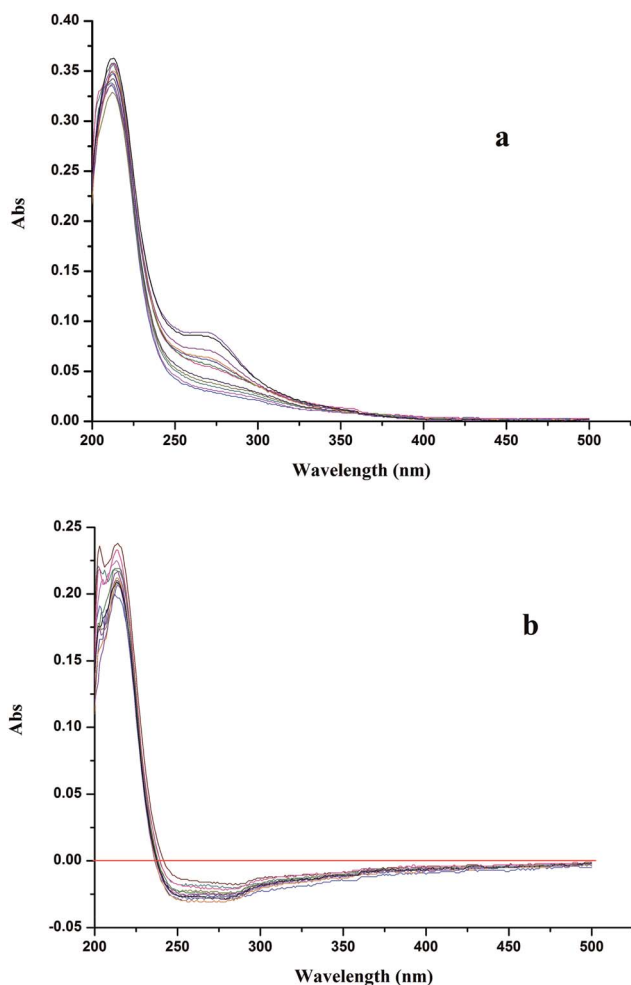


Fig. 3 (a) UV-vis (200–500 nm) absorption spectra of limonoid 2 (25 μM) in methanol after addition of ascending amounts of CuCl<sub>2</sub> (2–75 μmol L<sup>-1</sup>). (b) The differential spectra due to 2–Cu<sup>2+</sup> complex formation obtained by numerical subtraction from the above spectra of those of Cu<sup>2+</sup> and 2 at the corresponding concentrations.

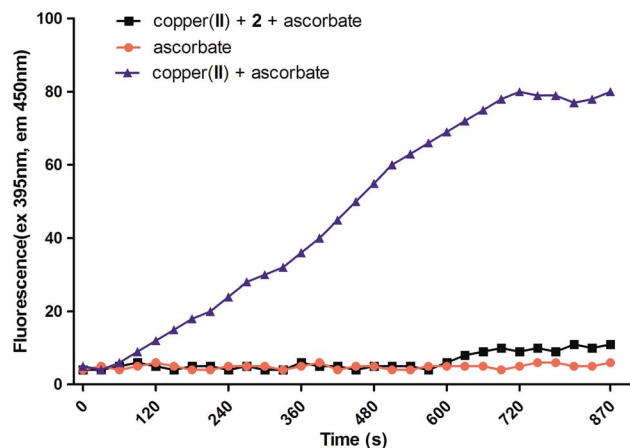


Fig. 4 Fluorescence intensity of the copper-ascorbate and copper-ascorbate-2 system. CCA (50 μM) and ascorbate (150 μM) were incubated in each system. Cu<sup>2+</sup> = 5 μM, ligand = 15 μM. PBS buffer, pH = 7.4.

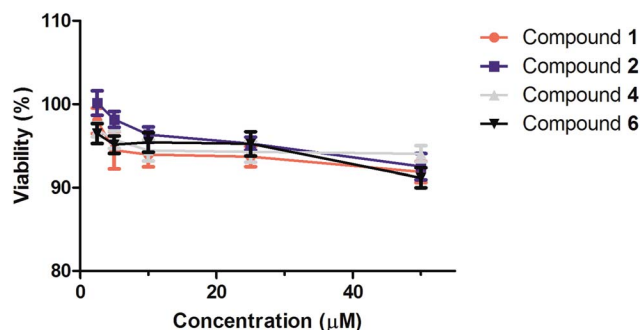


Fig. 5 Effects of limonoids on cell viability in SH-SY5Y cells. The cell viability was determined by the MTT assay after 24 h of incubation with various concentrations of limonoids 1, 2, 4 and 6. The results were expressed as a percentage of control cells. Values are reported as the mean ± SD of three independent experiments.

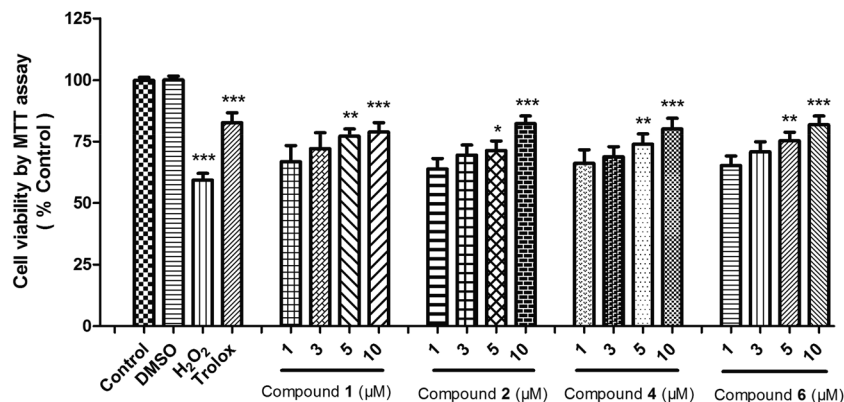


Fig. 6 Neuroprotection against H<sub>2</sub>O<sub>2</sub> toxicity. Limonoids 1, 2, 4 and 6 were tested for neuroprotective activity against H<sub>2</sub>O<sub>2</sub> toxicity in SH-SY5Y neuroblastoma cell cultures. Trolox (3 μM) was used as the reference compound. Results are expressed as percent viability compared to cells not treated with H<sub>2</sub>O<sub>2</sub>. Data represent the mean ± SD of three observations. \*\*\**p* < 0.001, \**p* < 0.05, \*\**p* < 0.01.

oxidative stress were measured by the human SH-SY5Y neuroblastoma cells.<sup>30</sup> Limonoids 1, 2, 4 and 6 were selected as representative compounds of different structure types. Firstly, the MTT assay was carried out to investigate the potential cytotoxicities of limonoids 1, 2, 4 and 6. As observed in Fig. 5, limonoids 1, 2, 4 and 6 did not show cytotoxic effects on cell viability at 1–50 μM after incubation for 24 h. It was suggested that limonoids 1, 2, 4 and 6 were nontoxicities to SH-SY5Y cells.

After that, the four selected limonoids were measured for capable of protecting human neuroblastoma cells (SH-SY5Y) against oxidative stress-associated cell death induced by H<sub>2</sub>O<sub>2</sub>. In the present assay, 100 μM H<sub>2</sub>O<sub>2</sub> was added to the growth medium and cell viability was reduced to 59.4% compared with control. The selected limonoids were added to the media at different concentrations immediately prior to the H<sub>2</sub>O<sub>2</sub> insult. Trolox was used as the reference compound. As indicated in Fig. 6, all limonoids exhibited neuroprotective effects against H<sub>2</sub>O<sub>2</sub>, which induced SH-SY5Y cell toxicity at different concentrations ranging from 1.25 to 10 μM. Limonoid 2 showed the highest protective capability (at 10 μM) almost the same as trolox at the concentration of 3 μM. This result indicated that the limonoids had the neuroprotective capability against oxidative stress.

## 4. Conclusion

Six new limonoids (1–6) and four known limonoids were isolated from the root bark of *D. angustifolius*. Their structures were established on the basis of extensive spectroscopic experiments. Bioactivity assays show that all limonoids exhibited metal chelating property and limonoid 2 could control Cu(II)-triggered hydroxyl radical (OH<sup>•</sup>) generation by halting copper redox cycling *via* metal complexation. In addition, the selected limonoids 1, 2, 4 and 6 were nontoxicity to SH-SY5Y cells and showed significant neuroprotective activity against neuronal death induced by oxidative stress. These findings suggested that limonoids from *D. angustifolius* such as limonoid 2 may be potential candidates for developing new drugs in the treatment

of neurodegenerative diseases, such as Alzheimer's disease and Parkinson's disease.

## Acknowledgements

We acknowledge the financial support by National New Drug Innovation Major Project of China (2011ZX09307-002-02), and Program Granted for Scientific Innovation Research of College Graduate in Jiangsu Province (CXZZ13\_0321).

## Notes and references

- 1 S. Hasegawa and M. Miyake, *Food Rev. Int.*, 1996, **12**, 413–435.
- 2 Q. Tian, E. G. Miller, H. Ahmad, L. Tang and B. S. Patil, *Nutr. Cancer*, 2001, **40**, 180–184.
- 3 G. Jayaprakasha, R. Singh, J. Pereira and K. Sakariah, *Phytochemistry*, 1997, **44**, 843–846.
- 4 D. E. Champagne, O. Koul, M. B. Isman, G. G. Scudder and G. Neil Towers, *Phytochemistry*, 1992, **31**, 377–394.
- 5 L. Lam, J. Zhang and S. Hasegawa, *Food Technol.*, 1994, **48**, 104–108.
- 6 S. Ejaz, A. Ejaz, K. Matsuda and C. W. Lim, *J. Sci. Food Agric.*, 2006, **86**, 339–345.
- 7 F. Xie, M. Zhang, C. F. Zhang, Z. T. Wang, B. Y. Yu and J. P. Kou, *J. Ethnopharmacol.*, 2008, **117**, 463–466.
- 8 E. M. Kurowska, C. Banh, S. Hasegawa and G. D. Manners, in *Citrus limonoids*, ed. M. A. Berhow, S. Hasegawa and G. D. Manners, ACS Symposium Series 758, USA, 2000, ch. 13, pp. 175–184.
- 9 H. Zhou, A. Hamazaki, J. D. Fontana, H. Takahashi, T. Esumi, C. B. Wandscheer, H. Tsujimoto and Y. Fukuyama, *J. Nat. Prod.*, 2004, **67**, 1544–1547.
- 10 T. Kikuchi, K. Ishii, T. Noto, A. Takahashi, K. Tabata, T. Suzuki and T. Akihisa, *J. Nat. Prod.*, 2011, **74**, 866–870.
- 11 P. Wang, J. B. Sun, J. Y. Xu, E. Z. Gao, Q. Yan, W. Qu, Y. L. Zhao and Z. G. Yu, *J. Chromatogr. B: Anal. Technol. Biomed. Life Sci.*, 2013, **942–943**, 1–8.

- 12 S. Hasegawa, M. Miyake and Y. Ozaki, *Biochemistry of citrus limonoids and their anticarcinogenic activity*, ACS symposium series, USA, 1994.
- 13 C. J. Yang, Y. J. Huang, C. Y. Wang, C. S. Wang, P. H. Wang, J. Y. Hung, T. H. Wang, H. K. Hsu, H. W. Huang and S. A. Kumar, *J. Med. Food*, 2010, **13**, 54–61.
- 14 J. S. Yoon, S. H. Sung and Y. C. Kim, *J. Nat. Prod.*, 2008, **71**, 208–211.
- 15 S. M. Poullose, E. D. Harris and B. S. Patil, *J. Nutr.*, 2005, **135**, 870–877.
- 16 G. S. Jeong, E. Byun, B. Li, D. S. Lee, R. B. An and Y. C. Kim, *Arch. Pharmacol. Res.*, 2010, **33**, 1269–1275.
- 17 T. S. Wu, C. Y. Li, Y. L. Leu and C. Q. Hu, *Phytochemistry*, 1999, **50**, 509–512.
- 18 J. B. Sun, W. Qu, F. Q. Guan, L. Z. Li and J. Y. Liang, *Chin. J. Nat. Med.*, 2014, **12**, 0222–0224.
- 19 J. B. Sun, X. Z. Wang, P. Wang, L. Z. Li, W. Qu and J. Y. Liang, *J. Ethnopharmacol.*, 2015, **159**, 296–300.
- 20 C. Hu, J. Han, J. Zhao, G. Song, Y. Li and D. Yin, *J. Integr. Plant Biol.*, 1989, **31**, 453–458.
- 21 J. B. Sun, W. Qu, Y. Xiong and J. Y. Liang, *Biochem. Syst. Ecol.*, 2013, **50**, 62–64.
- 22 J. B. Sun, W. Qu, P. Wang, F. H. Wu, L. Y. Wang and J. Y. Liang, *Fitoterapia*, 2013, **90**, 209–213.
- 23 M. Y. Lv, Y. Tian, Z. J. Zhang, F. G. Xu and J. B. Sun, *RSC Adv.*, 2015, **5**, 15700–15708.
- 24 P. Wang, J. B. Sun, E. Z. Gao, Y. L. Zhao, W. Qu and Z. G. Yu, *J. Chromatogr. B: Anal. Technol. Biomed. Life Sci.*, 2013, **928**, 44–51.
- 25 W. Huang, D. Lv, H. Yu, R. Sheng, S. C. Kim, P. Wu, K. Luo, J. Li and Y. Hu, *Bioorg. Med. Chem.*, 2010, **18**, 5610–5615.
- 26 R. Joseph, B. Ramanujam, A. Acharya, A. Khutia and C. P. Rao, *J. Org. Chem.*, 2008, **73**, 5745–5758.
- 27 L. Guilloreau, S. Combalbert, A. Sournia-Saquet, H. Mazarguil and P. Faller, *ChemBioChem*, 2007, **8**, 1317–1325.
- 28 M. Reddy, S. Majumdar and E. Harris, *Biochem. J.*, 2000, **350**, 855–863.
- 29 M. B. Hansen, S. E. Nielsen and K. Berg, *J. Immunol. Methods*, 1989, **119**, 203–210.
- 30 H. Zheng, M. B. Youdim and M. Fridkin, *J. Med. Chem.*, 2009, **52**, 4095–4098.
- 31 R. D. Bennett, S. Hasegawa and Z. Herman, *Phytochemistry*, 1989, **28**, 2777–2781.
- 32 N. T. Kipassa, T. Iwagawa, H. Okamura, M. Doe, Y. Morimoto and M. Nakatani, *Phytochemistry*, 2008, **69**, 1782–1787.
- 33 A. A. Zukas, A. P. Breksa III and G. D. Manners, *Phytochemistry*, 2004, **65**, 2705–2709.
- 34 S. M. Poullose, G. K. Jayaprakasha, R. T. Mayer, B. Girennavar and B. S. Patil, *J. Sci. Food Agric.*, 2007, **87**, 1699–1709.
- 35 R. Bennett and S. Hasegawa, *Tetrahedron*, 1981, **37**, 17–24.
- 36 R. L. Rouseff, *J. Agric. Food Chem.*, 1982, **30**, 504–507.
- 37 J. K. Rugutt, N. H. Fischer, M. A. Nauman, T. J. Schmidt and D. K. Berner, *Spectrosc. Lett.*, 1996, **29**, 711–726.
- 38 M. Nakatani, H. Takao, T. Iwashita, H. Naoki and T. Hase, *Phytochemistry*, 1988, **27**, 1429–1432.
- 39 A. I. Bush, *J. Alzheimer's Dis.*, 2008, **15**, 223–240.
- 40 J. Pierre and M. Fontecave, *BioMetals*, 1999, **12**, 195–199.
- 41 M. I. Fernández-Bachiller, C. Pérez, N. E. Campillo, J. A. Páez, G. C. González-Muñoz, P. Usán, E. García-Palomero, M. G. López, M. Villarroja and A. G. García, *ChemMedChem*, 2009, **4**, 828–841.
- 42 D. J. Bonda, X. Wang, G. Perry, A. Nunomura, M. Tabaton, X. Zhu and M. A. Smith, *Neuropharmacology*, 2010, **59**, 290–294.
- 43 P. Coleman, H. Federoff and R. Kurlan, *Neurology*, 2004, **63**, 1155–1162.